Available online at www.sciencedirect.com
SCIENCE DIRECT®
Journal of Solid State Chemistry 178 (2005) 185–193
JOURNAL OF SOLID STATE CHEMISTRY
www.elsevier.com/locate/jssc

Oxygen nonstoichiometry (δ) of $TiO_{2-\delta}$-revisited

D.-K. Lee[a,*], J.-I. Jeon[a], M.-H. Kim[b], W. Choi[c], H.-I. Yoo[a,1]

[a]Solid State Ionics Research Laboratory, School of Materials Science and Engineering, Seoul National University, San 56-1, Seoul 151742, Korea
[b]Department of Ceramic Science and Engineering, Changwon National University, Changwon 641-773, Korea
[c]School of Environmental Science and Engineering, POSTECH, Pohang 790-784, Korea

Received 12 December 2003; received in revised form 8 May 2004; accepted 15 July 2004

Abstract

Oxygen nonstoichiometry (δ) of "undoped" polycrystalline $TiO_{2-\delta}$ has been measured as a function of oxygen partial pressure in the widest ever examined range of $10^{-18} \leqslant P_{O_2}/\text{atm} \leqslant 10^{-1}$ at elevated temperatures ($1073 \leqslant T/\text{K} \leqslant 1473$) by thermogravimetry and coulometric titrometry combined and compared with all the reported values. Isothermal variation of nonstoichiometry against P_{O_2} is explained with a defect model involving quadruply ionized titanium interstitials, electrons, holes, and unidentified acceptors which may be background impurity acceptors or cation vacancies. The equilibrium constants for intrinsic electronic excitation reaction and redox reaction are determined from the nonstoichiometry measured and compared exhaustively with all the reported values. The relative partial molar enthalpy and entropy of oxygen are evaluated as functions of nonstoichiometry and the inner workings of their variations discussed.

Keywords: Oxygen nonstoichiometry; $TiO_{2-\delta}$; Thermogravimetry; Coulometric titration; Defect structure

1. Introduction

$TiO_{2-\delta}$ is an important technical material with applications such as photo-catalysts for water splitting [1,2], photo-electrodes for water photoelectrolysis [3] and gas sensors [4], to name only a few. Nonstoichiometry as a measure of the overall defect concentration or electronic carrier concentration is a crucial thermodynamic property to characterize for a better or optimal control of the functions of the oxide. Numerous studies have, thus, been carried out on the nonstoichiometry of rutile by using various techniques such as thermogravimetry [5–12], coulometric titration [13], electrical conductivity measurements [14–17], etc.

But, all the nonstoichiometry data are limited to $\delta > 10^{-4}$ or lower oxygen partial pressures (e.g., $P_{O_2} < 10^{-8}$ atm at 1000 °C). It is likely attributed to the then-available resolution of the experimental techniques employed. In order to get better and more insights into the defect chemistry of $TiO_{2-\delta}$, however, one may wish to extend the measurement into the range of $\delta < 10^{-4}$ or the higher oxygen partial pressure range (e.g., $P_{O_2} > 10^{-8}$ atm at 1000 °C). Furthermore, by doing that one may come closer to the inflection point on a nonstoichiometry isotherm which corresponds to the stoichiometric composition $\delta = 0$ and hence, allows one to determine more precisely the absolute values of nonstoichiometry [18].

In this paper, we measure the nonstoichiometry δ of nominally "undoped" $TiO_{2-\delta}$ as a function of oxygen partial pressure in the widest ever examined range, $10^{-18} \leqslant P_{O_2}/\text{atm} \leqslant 10^{-1}$ at elevated temperatures ($1073 \leqslant T/\text{K} \leqslant 1473$) via thermogravimetry and coulometric titrometry combined. The relevant defect equilibrium constants are subsequently estimated therefrom and exhaustively compared with all the reported ones. Finally, the partial molar quantities of oxygen are

*Corresponding author. Fax: +82-2-884-1413.
E-mail addresses: indeep@hanmail.net (D.-K. Lee), hiyoo@plaza.snu.ac.kr (H.-I. Yoo).
[1]Also for correspondence.

0022-4596/$ - see front matter © 2004 Elsevier Inc. All rights reserved.
doi:10.1016/j.jssc.2004.07.034

evaluated as a function of nonstoichiometry and the inner workings of redox reaction are discussed.

2. Experimental procedures

2.1. Specimens

Undoped polycrystalline samples of TiO_2 were prepared from commercially available rutile powder of 99.99% purity (Lot. 08604BF, Aldrich Co.) via a conventional ceramic processing route. The powder was pressed uniaxially under a pressure of ca. 5 MPa into rectangular as well as cylindrical pallets, followed by cold-isostatic pressing under 150 MPa. Sintering was subsequently carried out at 1450 °C in air atmosphere for 6 h. The as-sintered specimen was of more than 99% of the theoretical density with an average grain size of 11 ± 2 μm which is estimated by a line intercept method. For thermogravimetric analysis, the rectangular specimen was cut into parallelepipeds measuring ca. 3 mm × 3 mm × 29 mm.

2.2. Thermogravimetry

The TGA system used is based on a Cahn D-200 microbalance (Cahn Co., USA) with a sensitivity of 1 μg, which is schematically shown in Fig 1. It is noted that the two frameworks, one for the microbalance and the other for an electric furnace, are constructed separately in order to minimize vibration transfer. The entire system is placed on a vibration-proof pad in a room where temperature and humidity are kept constant at 22 ± 1 °C and 50 ± 2%, respectively, for the purpose of reducing the disturbances from environment.

A parallelepiped specimen (ca. 0.63 g) was hanged down from the microbalance to the reaction chamber with the aid of a Pt wire (0.2 mm thickness). The temperature of the reaction chamber was controlled within ±1 °C. Oxygen partial pressure around the specimen was controlled with N_2/O_2 and/or 90% N_2 + 10% CO/CO_2 gas mixtures and monitored by an in situ oxygen sensor based on yttria stabilized zirconia. The gas flow rate was fixed at 200 cm^3/min with the aid of a mass flow controller (MKS Inst. 5510, Germany) under a total pressure of 1 atm. Possible buoyancy and/or convection effect due to upward flow of gases fed from the bottom of the furnace were suppressed by inserting gas reflectors above the specimen inside the reaction chamber. The precision of the microbalance could thereby be maintained within ±1–2 μg in the conditions of present interest: $1073 \leqslant T/K \leqslant 1473$ and $10^{-18} \leqslant P_{O_2}/atm \leqslant 10^{-1}$.

Fig. 2 shows a typical procedure of measuring a relative weight change: Once the weight of the sample achieved a saturated value in a new oxygen partial pressure atmosphere, the gas flow was stopped for the purpose of eliminating the buoyancy force upon the specimen and then, its weight change, Δm from the initial weight m^* at the prefixed reference state was registered (i.e., $\Delta m = m_d - m_b$). The reference state was fixed at $P_{O_2} = 0.10$ atm at all temperatures examined.

The change of oxygen nonstoichiometry, $\Delta\delta$ relative to its reference value, δ^* at the starting point of thermogravimetry (corresponding to m^* at

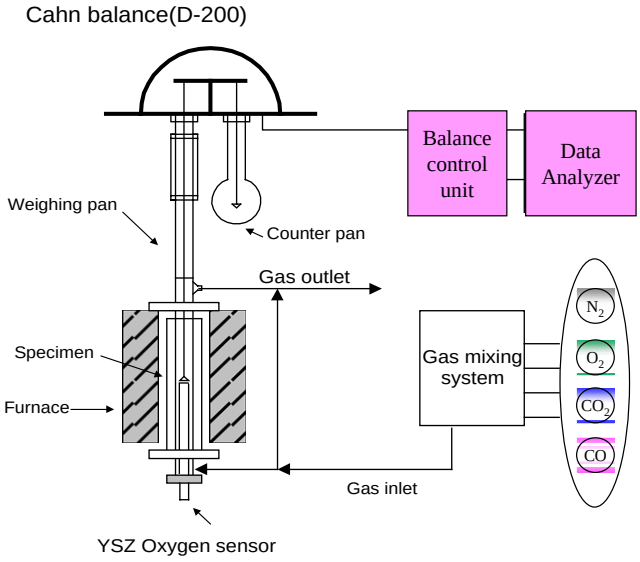

Fig. 1. Schematic of thermogravimetric analysis apparatus.

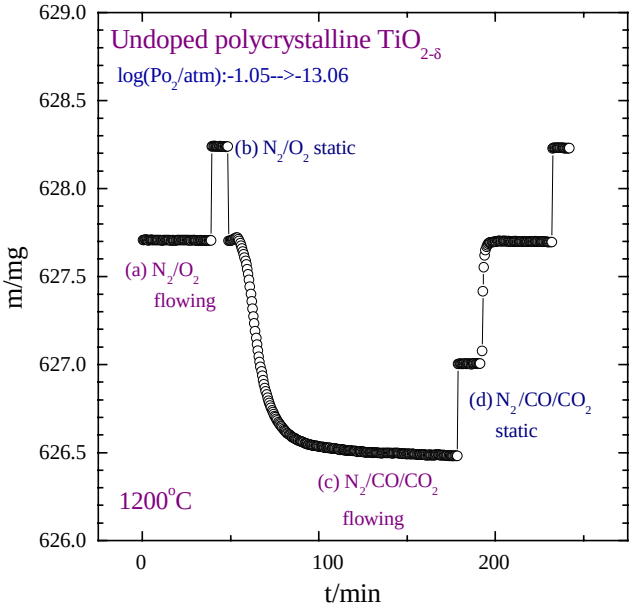

Fig. 2. Typical procedure of measuring the relative weight change by thermogravimetry.

$P_{O_2} = 0.10\,\text{atm}$) was calculated as

$$\Delta\delta = \delta - \delta^* = -\frac{M_{TiO_2}}{m^*}\frac{\Delta m}{M_O}, \quad (1)$$

where M_{TiO_2} and M_O denote the molar weight of TiO_2 and of atomic oxygen, respectively.

2.3. Coulometric titrometry

Coulometric titration was carried out in an electrochemical cell with the configuration,

$$\text{Pt},\ P_{O_2},\ TiO_{2-\delta}|ZrO_2(+8m/o\ Y_2O_3)|P^{ref}_{O_2},\ \text{Pt} \quad (2)$$

which is schematically shown in Fig. 3. For experimental details, the reader is referred to Ref. [19]. Briefly, a constant current, I in the range of 50–500 μA was passed through the YSZ electrolyte for a pre-fixed period of time t. The artifacts due to gas leakage, dead volume, possible reactions between the specimen and cell components, and nonstoichiometry change of the YSZ electrolyte itself, etc. were effectively eliminated or minimized [19]. A change in nonstoichiometry was determined as

$$\Delta\delta \equiv \delta - \delta^* = \frac{ItM_{TiO_2}}{2Fm^*}, \quad (3)$$

where F is the Faraday constant and δ^* denotes the oxygen deficit at the starting state of titration.

The equilibrium oxygen partial pressure around the specimen was determined from the open-circuit voltage, E, across the YSZ electrolyte (#1 in Fig. 3) or

$$E = \frac{RT}{4F}\ln\left(\frac{P_{O_2}}{P^{ref}_{O_2}}\right), \quad (4)$$

where $P^{ref}_{O_2}$ is the oxygen partial pressure of the reference gas flowing outside the titration cell. In the present work, CO_2/CO gas mixtures (with a mixing ratio of 30/1 to 1/15) were employed as the reference gas. If there were an appreciable mechanical or electrochemical leakage of oxygen gas through the cell under an oxygen potential difference, nonstoichiometry measurement would be subjected to an appreciable experimental error. Fig. 4 shows a temporal change of the open-circuit voltage E or due to Eq. (4), the oxygen partial pressure inside the cell while the oxygen partial pressure outside the cell being fixed at $\log(P^{ref}_{O_2}/\text{atm}) = -17.1$ and –18.8 at 900 and 800 °C, respectively. For about 10 h, little change is observed in oxygen partial pressure inside the cell from their initial values, $\log(P^{in}_{O_2}/\text{atm}) = -9.99$ and –1.02 at 900 and 800 °C, respectively, indicating that the electrochemical cell employed in the present work is essentially free from the artifact due to oxygen leakage across the cell.

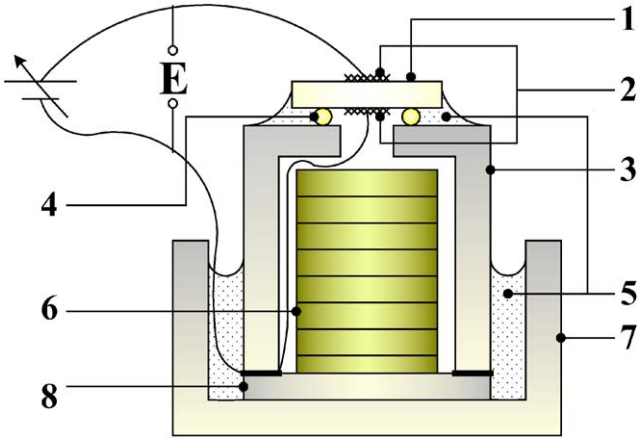

Fig. 3. Construction of coulometric titration cell. (1)YSZ electrolyte; (2) reversible electrode; (3) impermeable alumina cup; (4) gold-ring gasket; (5) borosilicate glass; (6) specimen tablets; (7) alumina crucible; and (8) alumina disk.

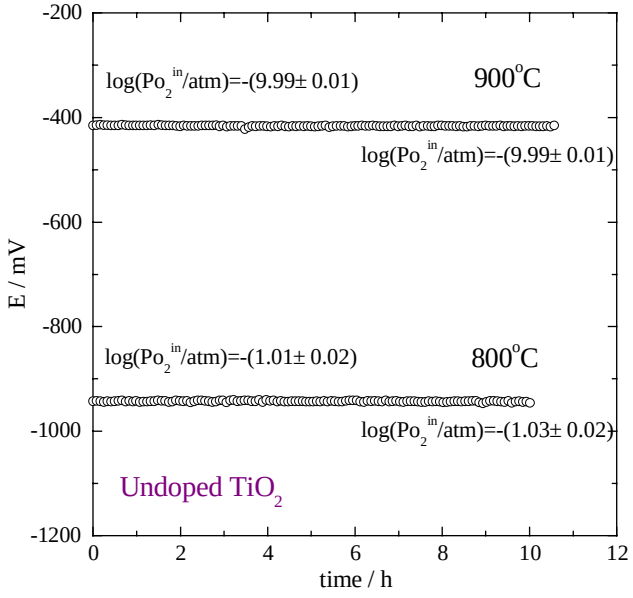

Fig. 4. Temporal change of the open-circuit voltage E across the YSZ while oxygen partial pressure outside is maintained at $\log(P^{ref}_{O_2}/\text{atm}) = -17.1$ and –18.8 at 900 and 800 °C, respectively.

The nonstoichiometry change relative to the reference value δ^* or, $\Delta\delta(=\delta-\delta^*)$ has been determined thereby as a function of oxygen partial pressure in the range of $10^{-18} \leqslant P_{O_2}/\text{atm} \leqslant 10^{-1}$ at different temperatures in the range of $1073 < T/\text{K} < 1273$. The reference states corresponding to δ^* were deliberately controlled to be close to that of thermogravimetry, i.e., $\log(P_{O_2}/\text{atm}) = -1.19$, -1.27 and -1.00 at 800, 900 and 1000 °C, respectively.

3. Results and discussions

In Fig. 5, the $\Delta\delta(=\delta-\delta^*)$ of $TiO_{2-\delta}$ as measured against oxygen partial pressure is shown at different temperatures by thermogravimetry (a) and coulometric

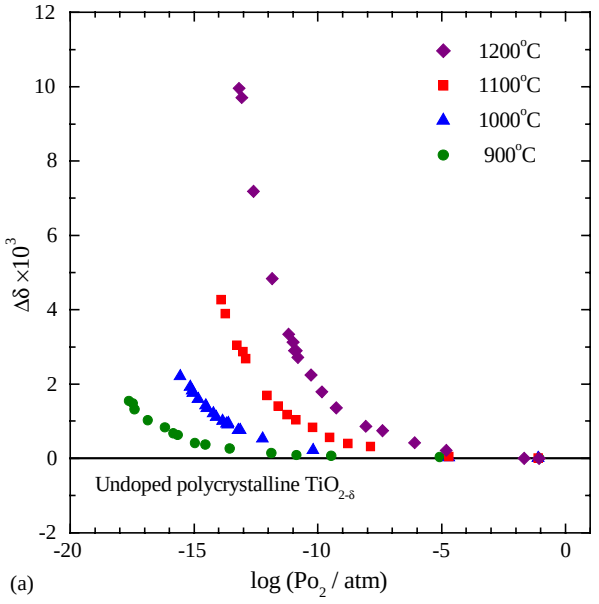

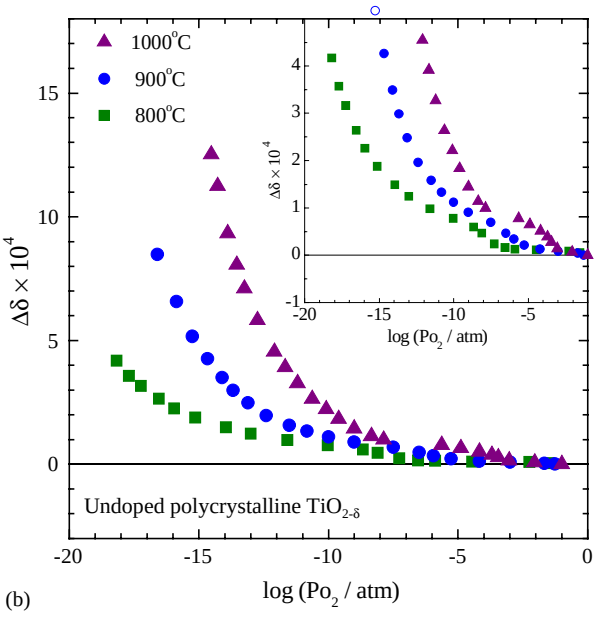

Fig. 5. Relative nonstoichiometry change, $\Delta\delta$ against oxygen partial pressure for undoped $TiO_{2-\delta}$ measured via: (a) thermogravimetry; and (b) coulometric titrometry.

titrometry (b), respectively. Upon comparison of the two, one can recognize that they generally appear to be in good agreement, but the $\Delta\delta$ isotherms by coulometric titrometry, in particular, each exhibit apparently an arrest at $\Delta\delta \approx 1 \times 10^{-4}$. It is noted that this nonstoichiometry change is beyond the detection limit of the thermobalance employed, and that the arresting behavior is highly systematic and reproducible. One may be tempted to ascribe the arrest to the appearance of the Magneli phases [20,21], but this possibility is ruled out because the latter appear only for $\delta > 0.006$ at, e.g., 1000 °C [20–25]. Similar arrests have ever been observed from Mn-doped $BaTiO_3$ due to the changes of valence of the multi-valent acceptors Mn with oxygen activity, [26] but its origin in the present case is not immediately clear.

Up to date, authors have generally agreed upon that $TiO_{2-\delta}$ is metal-excess (or oxygen-deficient), but, it remains unelucidated whether the metal-excess is attributed to Ti interstitials $Ti_i^{\bullet\bullet\bullet\bullet}$ [11–12,16,27–31] or oxygen vacancies $V_O^{\bullet\bullet}$ [5–6,17,32] or both. In the strictest sense, thus, one should take into account these two defect concentrations altogether in the analysis of the nonstoichiometry data. However, on the basis of our own experimental observation that the 4-probe d.c. electrical conductivity of the same specimen varies as $\sigma \propto P_{O_2}^{-m}$ with $m \approx 1/5$ (rather than 1/6) over most of the oxygen partial pressure range examined (see the inset in Fig. 7), we infer that $Ti_i^{\bullet\bullet\bullet\bullet}$, rather than $V_O^{\bullet\bullet}$, is in the majority. It is further noted that the trend of each isotherm in Fig. 5 suggests that an inflection point would come up soon, if not already passed, as P_{O_2} increased further over 1 atm. The inflection point on a $\Delta\delta$ isotherm corresponds to the stoichiometric composition ($\delta \approx 0$) where concentrations of electrons and holes are equal to each other ($n = p$) [18].

The defect structure of $TiO_{2-\delta}$ may then be described in terms of the following defect chemical scheme:

$$Ti_{Ti}^{\times} + 2O_O^{\times} = Ti_i^{\bullet\bullet\bullet\bullet} + 4e' + O_2(g);$$
$$K_{Ti} = [Ti_i^{\bullet\bullet\bullet\bullet}]n^4 P_{O_2}, \tag{5}$$

$$0 = e' + h^{\bullet}; \quad K_i = np, \tag{6}$$

$$n + [A'_C] = p + 4[Ti_i^{\bullet\bullet\bullet\bullet}], \tag{7}$$

where e' stands for free electrons, $h^{\bullet}$ free holes, A'_C unidentified effective acceptors that may be cation vacancies or background acceptor impurities, $[k]$ the concentration of the structure element k ($n = [e']$; $p = [h^{\bullet}]$), and K_j the equilibrium constant of the associated reaction j(= Ti, i) with the standard heat of reaction ΔH_j.

Subsequently, the nonstoichiometry or metal-excess δ of $TiO_{2-\delta}$ can be written as

$$\frac{N_A\delta}{V_m} = 2[Ti_i^{\bullet\bullet\bullet\bullet}] - \frac{1}{2}[A'] = \frac{1}{2}(n-p), \tag{8}$$

where N_A and V_m (= 18.8 $cm^3 mol^{-1}$) denote Avogadro's number and molar volume of the oxide, respectively. One associates Eqs. (5)–(7) and (8) to obtain an implicit equation for $\delta(= \Delta\delta + \delta^*)$ as

$$\log P_{O_2} = \log K_{Ti} - \log\left(\frac{\beta}{2}(\Delta\delta + \delta^*) + \frac{[A']}{4}\right) - 4\log\left(\beta(\Delta\delta + \delta^*) + \sqrt{(\beta(\Delta\delta + \delta^*))^2 + K_i}\right), \tag{9}$$

where $\beta \equiv N_A/V_m$.

The raw data, $\Delta\delta$ against $\log P_{O_2}$ are nonlinear-least-squares fitted to Eq. (9) and thereby, the absolute values for nonstoichiometry evaluated. The results are depicted by solid curves in Fig. 6. As is seen, Eq. (9) describes all the nonstoichiometry isotherms in Fig. 5 quite satisfactorily with the best estimated values for the fitting parameters K_i, K_{Ti} and $[A'_C]$ as listed in Table 1. It is confirmed that the results by the two different methods are in reasonable agreement despite the unexplained arrests on the isotherms by coulometric titrometry.

The oxygen partial pressure $P^o_{O_2}$ corresponding to $\delta = 0$ is evaluated from Eq. (9) at each temperature and listed in Table 1. The present $P^o_{O_2}$ values may have to be taken with caution because they have been evaluated with the data in not wide enough a hyperstoichiometric region ($\delta < 0$) and hence, they are likely subjected to somewhat larger uncertainty than the fitting errors themselves shown in the table. Nevertheless, it seems to be certain that the stoichiometric compositions fall well below 1 atm of oxygen partial pressure at the temperatures examined.

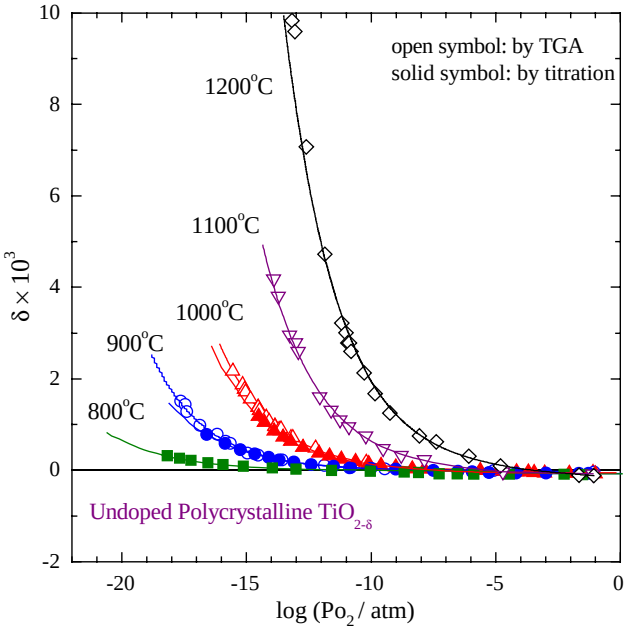

Fig. 6. Oxygen nonstoichiometry, δ vs. $\log(P_{O_2}/\text{atm})$ for undoped polycrystalline $TiO_{2-\delta}$ at different temperatures measured via thermogravimetry and coulometric titration, respectively. The solid lines are the best fits to Eq. (9) in the text.

All the literature data on the nonstoichiometry of undoped $TiO_{2-\delta}$ [5–8,11–13] are compiled and compared with the present one in Fig. 7, where $\log|\delta|$ is plotted vs. $\log P_{O_2}$ in order to represent the hyperstoichiometric values ($\delta < 0$) in the range of $P_{O_2} > P^o_{O_2}$ of the present study in particular. It is pointed out that all the

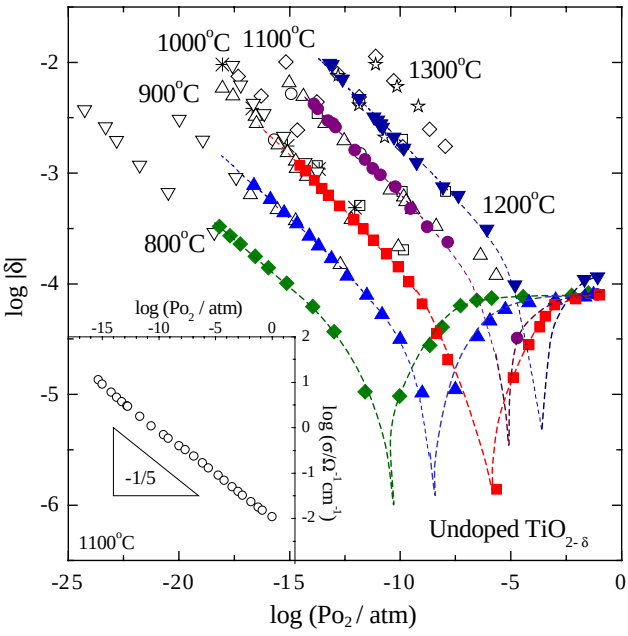

Fig. 7. Compilation of all the nonstoichiometry data $|\delta|$ reported on undoped $TiO_{2-\delta}$ including the present results: (○) Kofstad [5] by TGA; (□) Förland [6] by TGA; (◇) Moser et al. [7] by TGA; (+) Atlas and Schlehman [8] by gas analysis; (△) Marucco et al. [11] by TGA; (✻) Dirstine and Rosa [12] by TGA; (▽) Alcock et al. [13] by titrometry; (▼) this work at 1200 °C by TGA; (●) this work at 1100 °C TGA; (■) this work at 1000 °C by titrometry; (▲) this work at 900 °C by titrometry; (◆) this work at 800 °C by titrometry. Note that the two data sets by TGA and titrometry are in good agreement with each other at 900 and 1000 °C and hence, only the data by titrometry are presented. The dashed lines are for visual guidance. Inset, the electrical conductivity of the same specimen of TiO_2.

Table 1
The best-fitted values for $K_{Ti}/\text{atm}\,\text{cm}^{-15}$, K_i/cm^{-6}, and $[A']/\text{cm}^{-3}$ by thermogravimetry and coulometric titrometry, respectively, and the oxygen partial pressure $P^0_{O_2}$ corresponding to the stoichiometric composition ($\delta = 0$) of $TiO_{2-\delta}$

Temp. (°C)	$\log K_{Ti}/\text{atm}\,\text{cm}^{-15}$		$\log K_i/\text{cm}^{-6}$		$\log[A']/\text{cm}^{-3}$		$\log P^o_{O_2}/\text{atm}$	
	TGA	Titrometry	TGA	Titrometry	TGA	Titrometry	TGA	Titrometry
800	—	77.0±1.1		34.5±0.4	—	18.4±0.6	—	−(9.8±1.4)
900	81.64±0.05	81.47±0.09	34.86±0.15	35.98±0.07	18.41±0.06	18.76±0.07	−(5.9±0.3)	−(8.7±0.2)
1000	84.57±0.02	84.22±0.07	36.20±0.11	35.99±0.05	18.48±0.07	18.69±0.07	−(5.7±0.2)	−(5.9±0.1)
1100	87.55±0.07	—	37.3±1.2	—	18.68±0.2	—	−(5.1±2.4)	—
1200	89.92±0.05	—	37.7±0.2	—	18.88±0.14	—	−(3.7±0.4)	—

—: not available.

literature values for δ have been evaluated relative to air atmosphere, nevertheless, they are all in reasonable agreement with the present values, supporting the truth of the present $P^{o}_{O_2}$ values.

The present values for the redox reaction equilibrium constant, K_{Ti} of Eq. (5) are plotted against reciprocal temperature in Fig. 8 and compared with all the literature data [10–11,27,35]. It is seen that the present data by the two different methods are in reasonable agreement with the rest. The K_{Ti} values as determined from the present TGA data may best be represented as

$$K_{Ti}/\text{atm cm}^{-15} = \left(3.3^{+26.4}_{-0.4}\right) \times 10^{122} \times \exp\left(-\frac{(9.6 \pm 0.2)\text{eV}}{\text{kT}}\right). \quad (10)$$

For comparison as well as archival purpose, the reported values for the pre-exponential factor, $K_{Ti,0}$ and reaction enthalpy, ΔH_{Ti} of K_{Ti} [$=K_{Ti,0}\exp(-\Delta H_{Ti}/\text{kT})$] are all compiled in Table 2. The average ΔH_{Ti} value is 10.2 eV with a standard deviation of $\pm$0.7 eV.

The values for the intrinsic electron excitation reaction (Eq. 6), K_i as determined by the two different methods are compared in Fig. 9, where all the reported ones [33–34,36] are also shown. It is seen that the present two sets of data are not in good agreement with each other. Considering that K_i is determined predominantly by the nonstoichiometry in the stoichiometric region around $\delta = 0$ (see Eq. 9), their poor agreement is likely attributed, like the uncertainty with the $P^{o}_{O_2}$ values in Table 1, to a dearth of nonstoichiometry data in the sufficiently wide hyper-stoichiometric region ($\delta < 0$) in

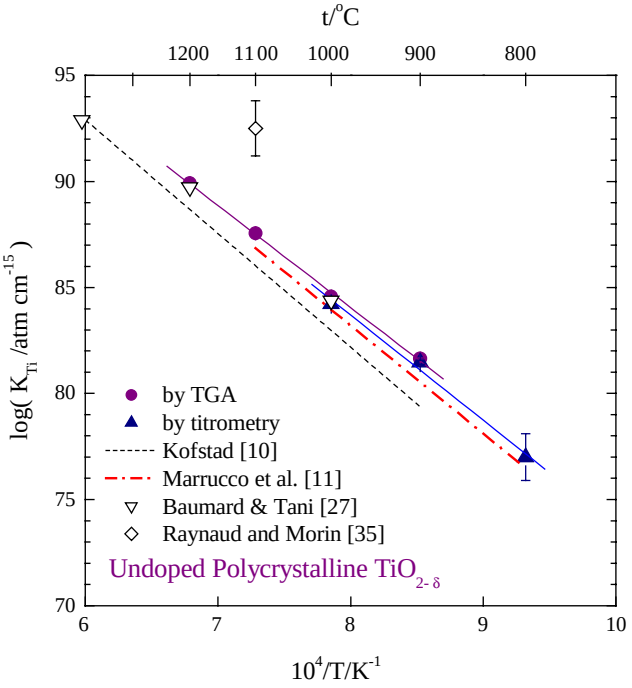

Fig. 8. The equilibrium constant for redox reaction (Eq. 5), K_{Ti} vs. reciprocal temperature for undoped $TiO_{2-\delta}$ including all the literature data.

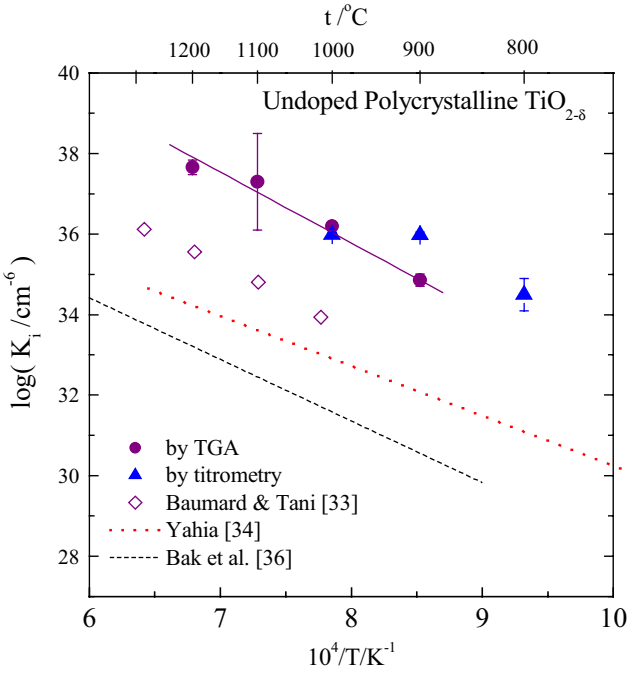

Fig. 9. The equilibrium constant for electron excitation reaction (Eq. 6), K_i vs. reciprocal temperature for undoped $TiO_{2-\delta}$ including all the literature data.

Table 2
Compilation of all the reported values for the pre-exponential factor and reaction enthalpy of K_{Ti} of TiO_2 such that $K_{Ti} = K_{Ti,o}\exp(-\Delta H_{Ti}/\text{kT})$

Authors	$K_{Ti,o}$/atm cm^{-15}	ΔH_{Ti}/eV	Measurement	Ref.
This work	$\left(3.3^{+26.4}_{-0.4}\right) \times 10^{122}$	9.6$\pm$0.2	Thermogravimetry	—
Kofstad	9.3×10^{124}	10.64	Thermogravimetry	[10]
Marucco et al.	1.1×10^{124}	10.14	Thermogravimetry	[11]
Baumard and Tani	$\left(2.1^{+330}_{-0.01}\right) \times 10^{120}$	9.0$\pm$0.6	Conductivity	[27]
Picard and Gerdanian	—	10.1	Thermogravimetry	[9]
Alcock et al.	—	10	Titrometry	[13]
Blumenthal et al.	—	10.67	Conductivity	[15]
Baumard and Tani	—	11.2	Thermopower	[33]

—: not available.

Fig. 6. For a precise determination of K_i by non-stoichiometry measurement, thus, one may have to enlarge the hyperstoichiometric region within the experimentally viable P_{O_2} range by, e.g., sufficiently doping acceptors. As a matter of fact, all the reported K_i values including the present ones show much larger scatter compared to K_{Ti} in Fig. 8. Notwithstanding the poor agreement among the magnitudes of K_i values, all the literature values for the band gap energies are averaged to be $\Delta H_i = 3.04 \pm 0.05$ eV [36]. The present data set by thermogravimetry gives a value $\Delta H_i = 3.3 \pm 0.3$ eV which is favorably compared with the average, but that by titrometry yields a much less precise value, 2.1 ± 1.1 eV, which is appreciably far off the average value. This seems to be ascribed to the nonstoichiometry arrests observed, see Fig. 5.

We will finally consider the partial molar quantities of component oxygen from the $\delta - P_{O_2} - T$ relation in Fig. 6. From the gas/solid equilibrium criterion, the relative partial molar Gibbs free energy of oxygen is written as

$$\Delta\bar{G}_O = \mu_O\,(s) - \tfrac{1}{2}\mu^o_{O_2}\,(g) = \tfrac{1}{2}RT\,\ln P_{O_2}, \tag{11}$$

where $\mu_O(s)$ and $\mu^o_{O_2}$ denote the chemical potential of component oxygen (O) in the solid oxide under the condition of interest and that of gas oxygen (O_2) at the standard state ($P_{O_2} = 1$ atm), respectively. The relative partial molar enthalpy, $\Delta\overline{H}_O$ and entropy, $\Delta\overline{S}_O$ of component oxygen are, thus, related to the equilibrium P_{O_2} as

$$\ln P_{O_2} = \frac{2\Delta\overline{H}_O}{RT} - \frac{2\Delta\overline{S}_O}{R}. \tag{12}$$

In Fig. 10 $\log(P_{O_2}/\text{atm})$ vs. reciprocal temperature is plotted at fixed compositions (δ). When two different P_{O_2} values (from the two different techniques) corresponded to a common nonstoichiometry value, their geometric mean was taken. As is seen, it is generally linear for a fixed δ over the temperature range examined. The relative partial molar enthalpy and entropy of oxygen may then be evaluated from the slope and intercept, respectively. The results are summarized in Figs. 11 and 12.

As is the case with $BaTiO_{3-\delta}$ [19], as δ increases or $TiO_{2-\delta}$ becomes exclusively n-type ($\delta \gg 0$ or $n \gg p$), $\Delta\bar{H}_O$ appears to saturate (to ca. –460 kJ mol^{-1}, see Fig. 11) and as δ gets close to 0, $\Delta\bar{H}_O$ varies rapidly. A similar trend is also observed with $\Delta\bar{S}_O$. These variations may be attributed to the difference in detailed oxygen incorporation reactions between the two branches of $TiO_{2-\delta}$, even though a distinct p-type branch is not identified in the δ isotherms obtained in this study:

$$Ti_i^{\bullet\bullet\bullet\bullet} + O_2\,(g) + 4e' = Ti_{Ti}^{\times} + 2O_O^{\times}, \tag{13a}$$

$$Ti_i^{\bullet\bullet\bullet\bullet} + O_2\,(g) = Ti_{Ti}^{\times} + 2O_O^{\times} + 4h^{\bullet} \tag{13b}$$

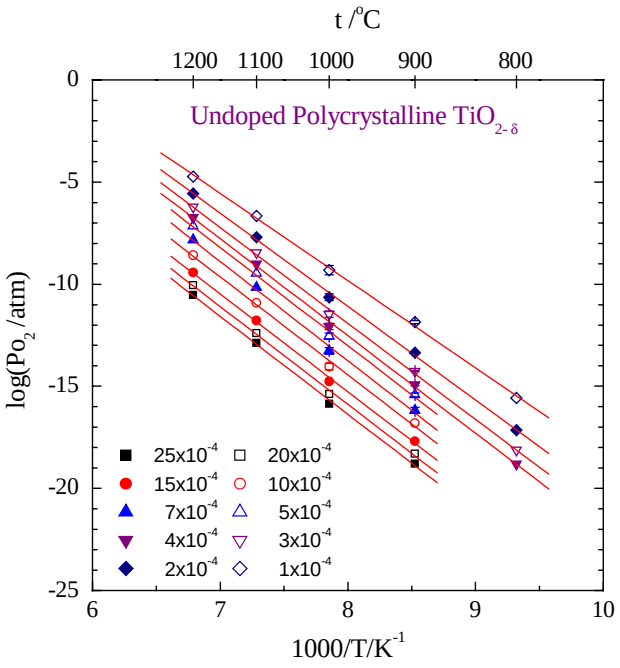

Fig. 10. Equilibrium oxygen partial pressure vs. reciprocal temperature at fixed nonstoichiometry values for undoped $TiO_{2-\delta}$.

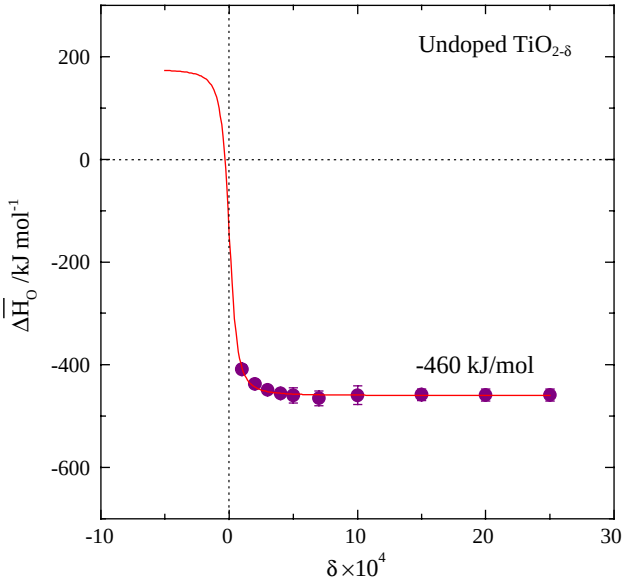

Fig. 11. The relative partial molar enthalpy, $\Delta\bar{H}_O$, of oxygen vs. nonstoichiometry δ. The solid curve is calculated on the basis of the ideal dilute solution model, Eq. (14) in the text.

in the hypostoichiometric n-type ($\delta \gg 0$) and hyperstoichiometric p-type ($\delta \ll 0$) branch, respectively. We have already presumed an ideal dilute solution behavior of defects in the present system. The partial molar enthalpy of component oxygen will, thus, have to be independent of δ in hypothetical p-type regime like n-type as expected from Fig. 11. According to Eqs. 13(a and b), the

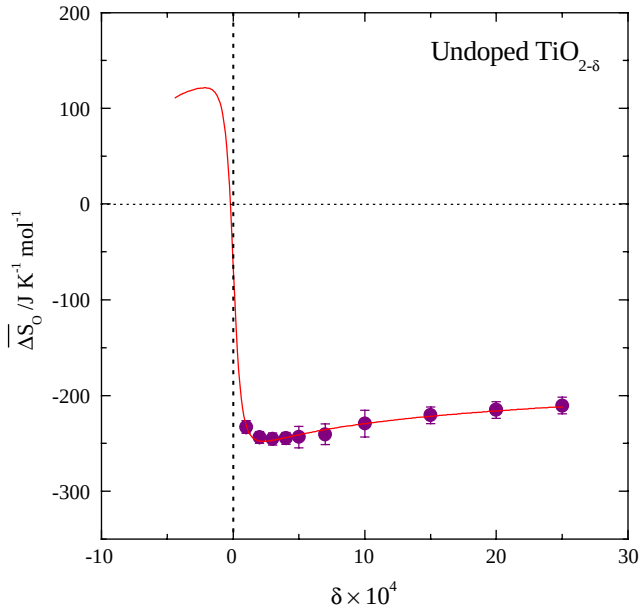

Fig. 12. The relative partial molar entropy, $\Delta\bar{S}_O$, of oxygen vs. nonstoichiometry δ. The solid curve is calculated on the basis of the ideal dilute solution model, Eq. (15) in the text.

difference in oxygen enthalpy between the n and p branches should be $\Delta\bar{H}_O(p) - \Delta\bar{H}_O(n) = 2\Delta\bar{H}_i$ i.e., 6.6 eV or 636 kJ mol^{-1} by taking the TGA result. In the n-to-p transition regime, $\Delta\bar{H}_O$ may then be given as the fractional sum of $\Delta\bar{H}_O(p)$ and $\Delta\bar{H}_O(n)$ or due to Eqs. (6) and (8),

$$\Delta\bar{H}_O = \frac{n}{n+p}\Delta\bar{H}_O(n) + \frac{p}{n+p}\Delta\bar{H}_O(p) = \frac{1}{2}[\Delta\bar{H}_O(p) + \Delta\bar{H}_O(n)] - \frac{\beta\delta}{[(\beta\delta)^2 + K_i]^{1/2}}\Delta H_i \quad (14)$$

with $\beta \equiv N_A/V_m (= 3.20 \times 10^{22}\,\mathrm{cm}^{-3})$. The $\Delta\bar{H}_O$ variation against δ is then fitted to Eq. (14) assuming K_i being constant over the temperature range of interest. The result is quite satisfactory as depicted by the solid curve in Fig. 11 yielding the best-fitted values, $\Delta\bar{H}_O(p) = 176 \pm 30\,\mathrm{kJmol}^{-1}$, $\Delta\bar{H}_O(n) = -460 \pm 30\,\mathrm{kJmol}^{-1}$ and $K_i = (4.6 \pm 0.5) \times 10^{36}\,\mathrm{cm}^{-6}$, respectively.

By the same argument, one can calculate $\Delta\bar{S}_O$ as

$$\Delta\bar{S}_O = \frac{n}{n+p}\Delta\bar{S}_O(n) + \frac{p}{n+p}\Delta\bar{S}_O(p) = \left(\frac{1}{2}S^o_{TiO_2} - \frac{1}{2}S^o_{Ti_i^{\bullet\bullet\bullet\bullet}} + S^o_p - S^o_n - \frac{1}{2}S^o_{O_2}\right) + \frac{1}{2}R\ln\left(\frac{1}{2}\delta + \frac{1}{4}\frac{[A'_C]}{\beta}\right) - (S^o_p + S^o_n - R\ln K_i)\frac{\beta\delta}{[(\beta\delta)^2 + K_i]^{1/2}} + R\ln\left(\frac{\beta\delta + [(\beta\delta)^2 + K_i]^{1/2}}{-\beta\delta + [(\beta\delta)^2 + K_i]^{1/2}}\right) \quad (15)$$

by using the relation

$$\bar{S}_k = S^o_k - R\ln[k] \quad (k = Ti_i^{\bullet\bullet\bullet\bullet}, p, n), \quad (16)$$

where S^o_k denotes the standard entropy of species k. Eq. (15) is fitted to the experimental data by using the value $K_i = 4.6 \times 10^{36}\,\mathrm{cm}^{-6}$ evaluated in Eq. (14) and $(\log[A'_C]/\mathrm{cm}^{-3}) = 18.6$ at 1000 °C in Table 1. The result is as depicted by the solid curve in Fig. 12 with the best estimated values

$$\tfrac{1}{2}S^o_{TiO_2} - \tfrac{1}{2}S^o_{Ti_i^{\bullet\bullet\bullet\bullet}} + S^o_p - S^o_n - \tfrac{1}{2}S^o_{O_2} = -(2 \pm 17)\mathrm{JK}^{-1}\,\mathrm{mol}^{-1},$$

$$S^o_p + S^o_n = 955 \pm 17\,\mathrm{JK}^{-1}\,\mathrm{mol}^{-1}.$$

Again, Eq. (15) well explains the variation of the partial molar entropy of component oxygen against nonstoichiometry.

4. Summary and conclusion

All the literature data up to date on the nonstoichiometry (δ) of $TiO_{2-\delta}$ have been limited to $\delta > 0.001$ or lower oxygen partial pressures (e.g., $P_{O_2} < 10^{-8}$ atm at 1000 °C). In the present study, we have extended, with a higher precision by thermogravimetry and coulometric titrometry combined, the measurement up to $P_{O_2} =$ 1 atm at temperatures in the range of 800–1200 °C. It is found that the stoichiometric composition ($\delta = 0$) falls below $P_{O_2} = 1$ atm at the temperatures examined. The nonstoichiometry can be explained in the defect chemical scheme involving quadruply charged Ti interstitials, electrons, holes and effective acceptors which may be background acceptor impurities or cation vacancies. The equilibrium constant of reduction reaction $Ti_{Ti}^{\times} + 2O_O^{\times} = Ti_i^{\bullet\bullet\bullet\bullet} + 4e' + O_2\,(g)$ is evaluated as $K_{Ti} = 3.3 \times 10^{122}\exp(-9.6\,\mathrm{eV/kT})\,\mathrm{atm\,cm}^{-15}$, which is in good agreement with the literature data. On the other hand, the equilibrium constant K_i for the intrinsic electronic excitation reaction, $0 = e' + h^{\bullet}$ cannot be evaluated with a sufficient precision mainly because of a dearth of nonstoichiometry data in the hyperstoichiometric region ($\delta < 0$). The relative partial molar enthalpy and entropy of component oxygen are evaluated as functions of nonstoichiometry, which are respectively found to be a sum of fractional contributions of oxygen incorporation reactions consuming electrons in the hypostoichiometric n-type branch ($\delta \gg 0$) and generating holes in the hyperstoichiometric p-type branch ($\delta \ll 0$), respectively, or $\Delta\mu_O = [n/(n+p)]\Delta\mu_O(n) + [p/(n+p)]\Delta\mu_O(p)$.

Acknowledgment

This work was supported by Korea Research Foundation Grant (KRF-2000-015-DS0028).

References

[1] A. Fujishima, K. Honda, Nature 238 (1972) 37.
[2] S.U.M. Khan, M. Al-Shahry, W.B. Ingler Jr., Science 297 (2002) 2243.
[3] A. Fujishima, K. Honda, Bull. Chem. Soc. Japan 44 (1971) 1148.
[4] T.Y. Tien, H.L. Stadler, E.F. Gibbsons, P.J. Zacmanidis, Am. Ceram Soc. Bull. 54 (1975) 280.
[5] P. Kofstad, J. Phys. Chem. Solids 23 (1962) 1579.
[6] K.S. Förland, Acta Chem. Scand. 18 (1964) 1267.
[7] J.B. Moser, R.N. Blumenthal, D.H. Whitmore, J. Am. Ceram. Soc. 48 (1965) 384.
[8] L.M. Atlas, G.J. Schlehman, Reported by Moser et al., J. Am. Ceram. Soc. 48 (1965) 384.
[9] C. Picard, P. Gerdanian, J. Solid State Chem. 14 (1975) 66.
[10] P. Kofstad, J. Less. Common. Met. 13 (1967) 635.
[11] J.-F. Marucco, J. Gautron, P. Lemasson, J. Phys. Chem. Solids. 42 (1981) 363.
[12] R.T. Dirstine, C.J. Rosa, Z. Metallkde. 70 (1979) 322.
[13] C.B. Alcock, S. Zador, B.C.H. Steele, Proc. Br. Ceram. Soc. 8 (1967) 231.
[14] D.S. Tannhauser, Solid. State. Commun. 1 (1963) 223.
[15] R.N. Blumenthal, J. Coburn, J. Baukus, W.M. Hirthe, J. Phys. Chem. Solids 27 (1966) 643.
[16] R.N. Blumenthal, J. Baukus, W.M. Hirthe, J. Electrochem. Soc. 114 (1967) 172.
[17] U. Balachandran, N.G. Eror, J. Mater. Sci. 23 (1988) 2676.
[18] C. Wagner, Prog. Solid State Chem. 6 (1971) 1.
[19] D.-K. Lee, H.-I. Yoo, Solid State Ionics 144 (2001) 87.
[20] P. Ehrlich, Z. Electrochem. 45 (1939) 362.
[21] S. Anderson, B. Collen, U. Kuilenstierna, A. Magneli, Acta Chem. Scand. 11 (1957) 1641.
[22] R.N. Blumenthal, D.H. Whitemore, J. Electrochem. Soc. 110 (1963) 92.
[23] J.S. Anderson, A.S. Khan, J. Less-Common Met. 22 (1970) 219.
[24] L.A. Bursill, B.G. Hyde, Prog. Solid State Chem. 7 (1972) 177.
[25] J.F. Baumard, D. Tanis, A.M. Anthony, J. Solid State Chem. 20 (1977) 43.
[26] D.-K. Lee, H.-I. Yoo, K.D. Becker, Solid State Ionics 154–155 (2002) 189.
[27] J.F. Baumard, E. Tani, J. Chem. Phys. 67 (1977) 857.
[28] N. Ait-Younes, F. Millot, P. Gerdanian, Solid State Ionics 12 (1984) 431.
[29] K. Hoshino N.L. Peterson, C.L. Willey, J. Phys. Chem. Solids 46 (1985) 1977.
[30] V.N. Bogomolov, I.A. Smirnov, E.V. Shadrivhev, Sov. Phys. Solid State 11 (1970) 2606.
[31] J. Sasaki, N.L. Peterson, K. Hoshino, J. Phys. Chem. Solids 46 (1985) 1267.
[32] E.H. Greener, F.J. Barone, W.M. Hirthe, J. Am. Ceram. Soc. 48 (1965) 623.
[33] J.F. Baumard, E. Tani, Phys. Stat. Sol. (a) 39 (1977) 373.
[34] J. Yahia, Phys. Rev. 130 (1963) 1711.
[35] G.M. Raynaud, F. Morin, J. Phys. Chem. Solids 46 (1985) 1371.
[36] T. Bak, J. Nowotny, M. Rekas, C.C. Sorrell, J. Phys. Chem. Solids 64 (2003) 1043.